

Biofabrication



PAPER

RECEIVED
30 July 2018

REVISED
25 September 2018

ACCEPTED FOR PUBLICATION
3 October 2018

PUBLISHED
30 October 2018

Engineering of microscale vascularized fat that responds to perfusion with lipoactive hormones

Xuanyue Li¹, Jingyi Xia¹, Calin T Nicolescu¹, Miles W Massidda¹, Tyler J Ryan¹ and Joe Tien^{1,2}

¹ Department of Biomedical Engineering, Boston University, Boston, MA 02215, United States of America

² Division of Materials Science and Engineering, Boston University, Brookline, MA 02446, United States of America

E-mail: jtien@bu.edu

Keywords: microvascular tissue engineering, collagen, microfluidic vascularization, Intralipid, microphysiological system

Abstract

Current methods to treat large soft-tissue defects mainly rely on autologous transfer of adipocutaneous flaps, a method that is often limited by donor site availability. Engineered vascularized adipose tissues can potentially be a viable and readily accessible substitute to autologous flaps. In this study, we engineered a small-scale adipose tissue with pre-patterned vasculature that enables immediate perfusion. Vessels formed after one day of perfusion and displayed barrier function after three days of perfusion. Under constant perfusion, adipose tissues remained viable and responded to lipoactive hormones insulin and epinephrine with lipid accumulation and loss, respectively. Adipocyte growth correlated inversely with distance away from the feeding vessel, as predicted by a Krogh-type model.

1. Introduction

Large soft-tissue defects often accompany traumatic injury, tumor resection, or diabetic foot. The current gold standard for reconstruction of these defects is autologous tissue transfer of adipocutaneous flaps [1]. This technique is limited by tissue availability and may result in donor-site morbidity. The engineering of a stable and functional adipose tissue that can be grafted as a perfused unit could be invaluable for treating soft-tissue defects [2, 3].

Studies have shown that immediate perfusion is absolutely required for survival of free flaps and transplanted tissue, unless the tissue is extremely thin [4, 5]. Free fat grafting by lipoinjection, which disrupts the native adipose vasculature and cannot establish immediate perfusion, often fails to maintain volume over time [6, 7]. Therefore, it is crucial for engineered adipose tissue to not only have a preformed vasculature, but one that is perfused. Most studies to engineer vascularized fat tissue have employed a combination of angiogenic and adipogenic growth factors, a suspension of endothelial cells (ECs) and adipocytes and/or adipocyte progenitors, and an appropriate scaffold [8–10]. The vasculature in these engineered tissues forms by angiogenesis and/or vasculogenesis, which typically require one or more weeks and can yield a poorly organized microvascular network.

Moreover, the small diameter of these microvessels makes cannulation and surgical anastomosis impossible, and it is unclear how to establish perfusion during tissue maturation *in vitro* and upon grafting *in vivo*. Insertion of an arteriovenous bundle into the developing construct can provide a vascular pedicle for surgical anastomosis, but even here, generation of vascularized fat requires weeks [11].

With few exceptions, studies of engineered adipose tissue have focused primarily on characterizing the structure of the tissue histologically and have confirmed the presence of adipocytes by staining with lipid markers such as Oil Red O [12]. Along with its structural role, however, adipose tissue plays critical metabolic and endocrine roles that depend on signals from adjacent ECs that line their lumens [13]. Insulin has been shown to upregulate lipogenesis both by increasing uptake of free fatty acid [14] and by increasing conversion of triacylglycerol into fatty acid by lipoprotein lipase that is expressed on the surface of ECs [15]. Conversely, β -adrenergic agonists such as epinephrine have been shown to upregulate lipolysis by stimulating the activity of hormone-sensitive lipase [16]. It is important to demonstrate that engineered adipose tissue responds to lipoactive hormones in a physiologically relevant manner [17].

The objective of the current study was to engineer a vascularized adipose tissue that could be immediately

and constantly perfused and that demonstrated lipoactivity. The methods described here built upon previously described techniques to vascularize microfluidic collagen scaffolds [18], and yielded a ‘fundamental unit’ of adipose tissue that contained one microvessel that perfused an adipocyte-laden collagen gel. We showed that the microvessel within the engineered adipose tissue possessed good barrier function, and that the adipocytes responded appropriately to vascular perfusion with lipoactive hormones.

2. Methods

2.1. Cell culture

Mouse 3T3-L1 preadipocytes (ATCC) were grown in high-glucose DMEM (Invitrogen) supplemented with 10% heat-inactivated fetal bovine serum (FBS; Atlanta Biologicals) and 1% glutamine-penicillin-streptomycin (GPS; Invitrogen) (‘basal medium’). The 3T3-L1 cells were routinely passaged at 1:10 ratio and were used up to passage nine.

To differentiate 3T3-L1 cells, we switched cultures two days post-confluence, to ‘differentiation medium’: basal medium supplemented with 0.25 μM dexamethasone, 2 μM rosiglitazone, 10 $\mu\text{g ml}^{-1}$ insulin, 0.5 mM 3-isobutyl-1-methylxanthine, and 0.2 mM ascorbic acid 2-phosphate (all from Sigma) [19]. After another two days, differentiation medium was replaced with ‘maintenance medium’: basal medium supplemented with 10 $\mu\text{g ml}^{-1}$ insulin only.

Human dermal microvascular ECs (PromoCell) were grown on gelatin-coated dishes in MCDB131 medium (Caisson) that was supplemented with 10% FBS, 1% GPS, 1 $\mu\text{g ml}^{-1}$ hydrocortisone (Sigma), 80 μM dibutyryl cyclic AMP (Sigma), 25 $\mu\text{g ml}^{-1}$ EC growth supplement (Alfa Aesar), 2 U ml^{-1} heparin (Sigma), and 0.2 mM ascorbic acid 2-phosphate (‘EC culture medium’). ECs were routinely passaged at a 1:4 ratio and were used up to passage nine.

2.2. Formation of vascularized adipose tissues

Adipose tissues that contained a single microvessel ($n = 57$) were formed using a modified procedure from a previous study [18]. Briefly, a stainless steel needle of 120 μm in diameter (Seirin) was positioned at the center of a 1 mm \times 1 mm \times 7 mm chamber in silicone (PDMS) mold. Rat tail type I collagen (diluted to 6 mg ml^{-1} before mixing with cells; Corning) was neutralized to pH 7. Confluent 3T3-L1 cells were trypsinized 6–7 days after start of differentiation and centrifuged at $\sim 120 \text{ g}$ for three minutes, yielding a cell pellet that was $\sim 15 \mu\text{l}$. The cell pellet was gently mixed with 375 μl neutralized collagen to yield a density of $\sim 10^6 \text{ cells ml}^{-1}$, and was gelled for thirty minutes at room temperature in the chamber around the needle; the final concentration of collagen was $\sim 5.8 \text{ mg ml}^{-1}$. This collagen concentration was high enough to inhibit vascular sprouting [18] without limiting

adipocyte growth. The needle was removed, and the resulting channel was then seeded with ECs. Perfusion was set up in the microscale tissue by connecting each end of the channel to a reservoir of EC culture media that was supplemented with 3% dextran (70 kDa; Sigma) (‘perfusion media’). A pressure difference of 4.5 cm H₂O was maintained for up to seven days. Perfused adipose tissues were kept at 37 °C in 5% CO₂ and refed twice daily (figure 1). As a control, some gels ($n = 8$) were formed and vascularized without the addition of adipocytes.

To form larger tissues ($n = 17$), we used wider chambers (1 mm \times 11 mm \times 6 mm) to hold the needle; the needle was placed 0.5 mm away from one edge of the chamber before adding the adipocyte-containing collagen. Here, the cell density was $10^6 \text{ cells ml}^{-1}$ or $1.5 \times 10^6 \text{ cells ml}^{-1}$.

2.3. Hydraulic permeability and stiffness assays

To measure the hydraulic permeability of adipocyte-containing and cell-free collagen gels, we gelled collagen with and without $10^6 \text{ 3T3-L1 cells ml}^{-1}$ in PDMS molds to form 1 mm \times 1 mm \times 7 mm solid gels. On days 1 through 5 after gelling, perfusion media that was supplemented with 10 $\mu\text{g ml}^{-1}$ insulin and 0.5 mg ml^{-1} Intralipid (Sigma) was allowed to flow through the gel for two hours under an applied pressure difference of 1–1.1 cm H₂O. The hydraulic permeability coefficient k was calculated using equation (1), where Q is the flow rate of the media, A is the cross-sectional area of the gel, ΔP is the pressure difference, and L is the length of the gel:

$$k = \frac{QL}{A\Delta P}. \quad (1)$$

To measure the stiffness of adipocyte-containing and cell-free collagen gels, we formed disc-shaped collagen gels with and without $10^6 \text{ 3T3-L1 cells ml}^{-1}$ in a cylindrical mold that was 6 mm in diameter and 2 mm in height. Gels were again kept in perfusion media that was supplemented with 10 $\mu\text{g ml}^{-1}$ insulin and 0.5 mg ml^{-1} Intralipid. On days 1, 3, and 5 after gelling, each gel was submerged horizontally in phosphate-buffered saline (PBS), and an aluminum ball with diameter of 1.6 mm (Precision Balls) was placed on the upper surface of the collagen. After one hour, the indentation of the aluminum ball was measured, and the stiffness was calculated as indentation modulus using equation (2), where R and ρ are the radius and density of the aluminum ball, respectively, ρ_{PBS} is the density of PBS, δ is the indentation depth, and g is 9.8 m s⁻² [20]:

$$E = \frac{\pi R^{5/2}(\rho - \rho_{\text{PBS}})g}{\delta^{3/2}}. \quad (2)$$

2.4. Lipogenesis and lipolysis assay

After vascularized adipose tissues were perfused for one day, the perfusion media was supplemented with

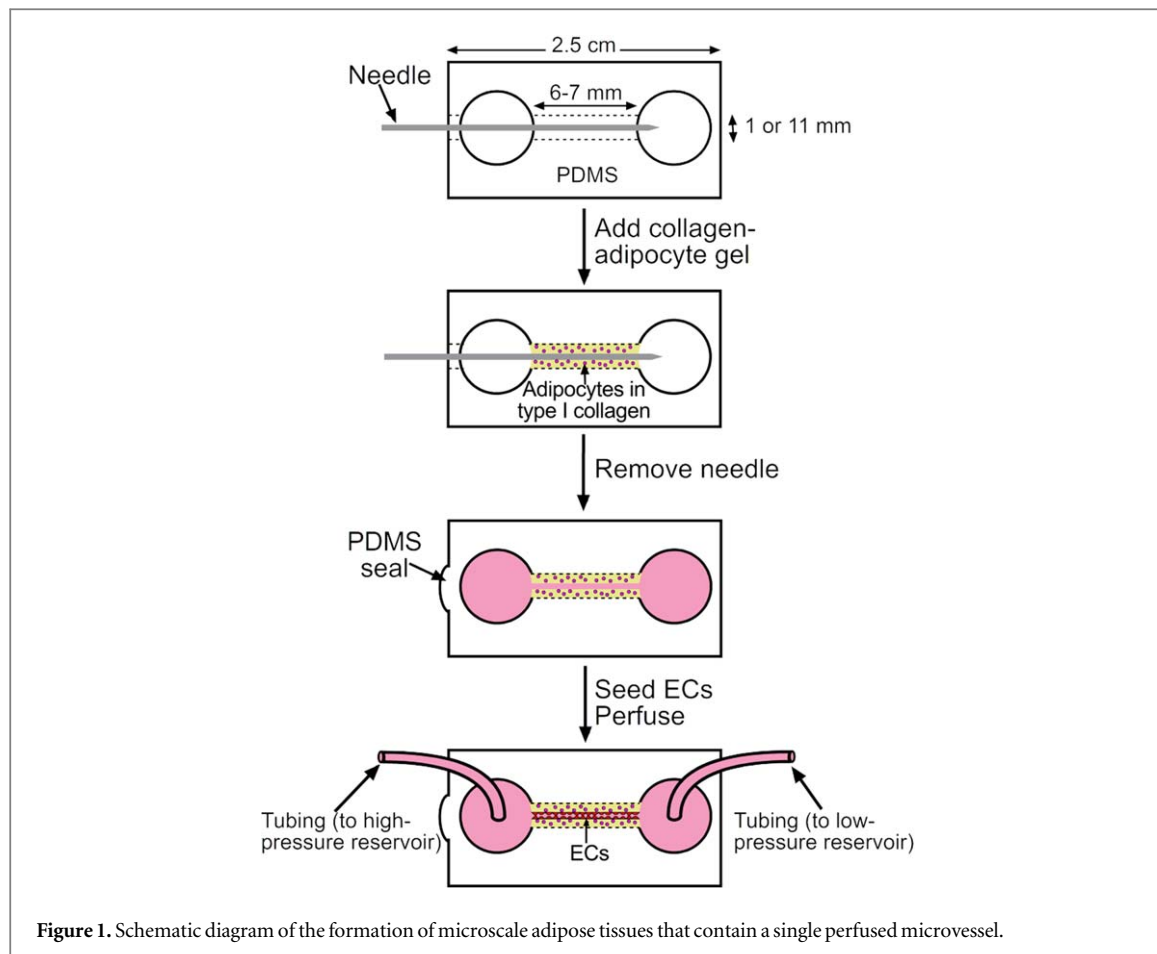


Figure 1. Schematic diagram of the formation of microscale adipose tissues that contain a single perfused microvessel.

10 $\mu\text{g ml}^{-1}$ insulin and 0.5 mg ml^{-1} Intralipid. Intralipid is an emulsion of lipid that is used for parenteral nutrition and has been shown to increase the accumulation of lipids in adipocytes in planar culture [21]. After another four days of perfusion (i.e., on day 5 of perfusion), tissues were then switched to perfusion with insulin- and Intralipid-free media with or without 10 μM epinephrine for an additional four days (i.e., to day 9 of perfusion). Phase-contrast images were taken on days 1, 3, 5, 7, and 9 of perfusion, and the lipid droplet area per cell was measured manually for 30–40 adipocytes per tissue. The results were compared between tissues with or without insulin/Intralipid for days 1–5 and between tissues with or without epinephrine for days 5–9. Images were obtained with a 10 \times /0.30 Plan-Neofluar objective on a Zeiss Axiovert 200M microscope at 1300 \times 1030 camera resolution. All lipid droplet measurements were performed in a blinded manner.

Wide tissues that contained 10^6 or 1.5×10^6 3T3-L1 cells ml^{-1} and a single vessel were perfused for seven days, the last six with media that was supplemented with 10 $\mu\text{g ml}^{-1}$ insulin and 0.5 mg ml^{-1} Intralipid. On days 1, 3, 5, and 7 of perfusion, phase-contrast images of adipocytes that were at different distances from the vessel (0–1 mm, 1–2 mm, etc) were taken, and the lipid droplet area per cell of 30–40 cells were measured for each distance range.

2.5. Vascular permeability assay

Macromolecular permeability of the endothelium in vascularized tissue was measured using a previous method [22]. Briefly, after 3–4 days of perfusion, media in the upper reservoir was replaced with perfusion media that was supplemented with 50 $\mu\text{g ml}^{-1}$ Alexa Fluor 594-conjugated bovine serum albumin (BSA) and 20 $\mu\text{g ml}^{-1}$ Alexa Fluor 488-conjugated 10 kDa dextran (both from Invitrogen). The tissue was placed in an environmental chamber at 37 °C, and time-lapse images were captured every minute for thirty minutes in both red and green channels. Average gray values for the time-lapse images were measured using ImageJ and recorded. Permeability coefficients were determined using an algorithm to correct for the non-instantaneous filling of the vessel by fluorescent media [23].

2.6. Adipocyte viability assay

Adipose tissues were disconnected from tubing after three days of perfusion. Perfusion media containing 10 $\mu\text{g ml}^{-1}$ calcein AM, 10 μM ethidium homodimer, and 5 $\mu\text{g ml}^{-1}$ Hoechst 33342 (all from Invitrogen) was added to the wells on either side of the tissue, allowed to flow through the vessel, and incubated for thirty minutes at 37 °C. To first visualize viability of ECs, we captured images in green, red, and blue channels for live cells, dead cells, and nuclei, respectively, while focusing at the microvessel. The tissues

were then carefully taken out of the PDMS mold and submerged in media containing live/dead stain for another thirty minutes. To visualize live and dead adipocytes, we captured images using the same excitation wavelengths while focusing on adipocytes in the collagen gel.

2.7. Staining

After one day of perfusion, the engineered tissues were fixed by perfusion with 4% paraformaldehyde (15 min, 20 °C). Each tissue was then blocked and permeabilized with 5% goat serum and 0.5% Triton X-100 in PBS ('blocking buffer') for at least one hour. To stain for the endothelial junctional marker CD31, we perfused the permeabilized tissue with 5 µg ml⁻¹ mouse anti-human CD31 (clone WM-59; Sigma) for one hour, flushed the tissue three times for twenty minutes each with blocking buffer, perfused the tissue with 10 µg ml⁻¹ Alexa Fluor 488-conjugated goat anti-mouse IgG (Invitrogen) for one hour, and flushed the tissue three times for twenty minutes each with blocking buffer. The tissue was then taken out of the PDMS chamber and stained for lipid droplets with 25 µg ml⁻¹ Nile Red (Sigma). Stained tissue was imaged in green and red channels for visualization of CD31 and lipid droplets, respectively. To acquire cross-sectional views, we embedded the stained tissue in 4% agarose, sliced it into 0.5–1 mm thick pieces, and imaged at the lumen.

2.8. Statistics

All statistical tests were performed using Graphpad Prism ver. 6. Kruskal-Wallis test with Dunn's multiple comparison was used to compare solute selectivities or permeability coefficients to BSA and dextran. Two-way ANOVA with Bonferroni post-test was used to compare hydraulic permeabilities, indentation moduli, or lipid droplet areas per cell. To determine if hydraulic permeabilities and indentation moduli varied over time, we performed a linear fit on data collected on different days and the slope was compared to zero. A value of $p < 0.05$ was considered statistically significant. Data are listed as means \pm standard deviation.

3. Results

3.1. Addition of adipocytes increases hydraulic permeability and decreases stiffness of collagen gels

Compared to bare collagen gels, adipocyte-containing gels displayed lower indentation moduli (166–189 Pa versus 278–291 Pa, measured on days 1, 3, and 5 after gelling, $p < 0.001$ for all days, figure 2(A)), and higher hydraulic permeabilities ($8.6\text{--}10.1 \times 10^{-8}$ cm⁴ dyn⁻¹ s⁻¹ versus $5.3\text{--}6.7 \times 10^{-8}$ cm⁴ dyn⁻¹ s⁻¹, measured on days 1–5 after gelling, $p < 0.05$ for all days except day 3, figure 2(B)). Elastic moduli and hydraulic

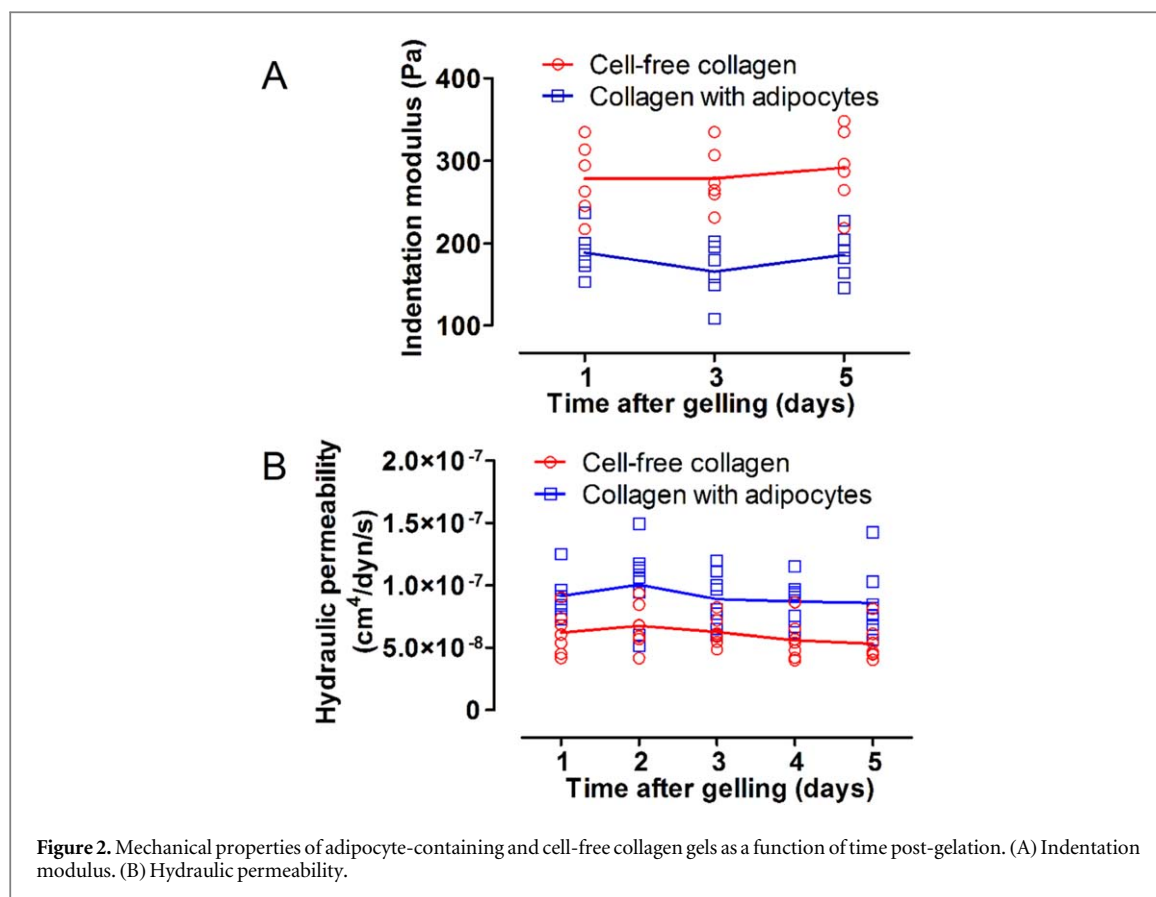
permeabilities did not vary significantly with time, for both cell-free and adipocyte-containing collagen gels ($p = 0.59$ and 0.88 for moduli and $p = 0.12$ and 0.33 for hydraulic permeability, for cell-free and cell-laden gels, respectively).

3.2. Engineered adipose tissues possess functional vasculature and remain viable

ECs that were seeded in a channel within an adipocyte-containing gel reached confluence within one day of perfusion. The channel diameter expanded from 120 to ~ 190 µm over 2–3 days, and stabilized at this larger size (figure 3(A)). The flow rate was initially ~ 0.5 ml h⁻¹ and increased to 1.6 ± 0.3 ml h⁻¹ after the channel widened.

Staining for the EC junctional protein CD31 showed that the engineered tissue possessed confluent endothelium after one day of perfusion (figure 3(B)). We observed that the diameter of the vessels that were formed in adipocyte-containing gels varied across the lengths of the vessels. This result is in contrast to vessels that were formed in adipocyte-free collagen gel, which possessed smoothly tapering lumens across their lengths [18, 24]. The presence of adipocytes was confirmed by staining for neutral lipid with Nile Red (figure 3(B)). To prove that the adipocytes were viable, we stained the tissue with calcein AM and ethidium homodimer (figure 3(C)). We found a viability rate of $>99\%$ ($n = 3$) for ECs and $93 \pm 3\%$ ($n = 5$) for adipocytes after three days of perfusion.

To characterize the barrier function of the vessels, we carried out permeability assays on vessels in adipocyte-free collagen gels and in adipocyte-containing collagen gels that were perfused under standard conditions, and in adipocyte-containing collagen gels that were perfused with media that was supplemented with 10 µg ml⁻¹ insulin and 0.5 mg ml⁻¹ Intralipid starting from day 1 of perfusion (figures 3(D)–(F)). Permeability coefficients for BSA for these three conditions were: $(9.0 \pm 3.4) \times 10^{-7}$ cm s⁻¹, $(2.7 \pm 1.0) \times 10^{-6}$ cm s⁻¹, and $(2.6 \pm 1.0) \times 10^{-6}$ cm s⁻¹, respectively (figure 3(E)). Vessels that were formed in adipocyte-containing gels exhibited a three-fold increase in permeability to BSA compared to vessels in adipocyte-free gels, regardless of the presence of insulin and Intralipid ($p < 0.001$ for adipocyte-free versus adipocyte-containing without supplements, $p < 0.01$ for adipocyte-free versus adipocyte-containing with supplements). Perfusion with insulin and Intralipid did not change vessel permeability in adipocyte-containing gels ($p = 0.81$, figure 3(E)). Permeabilities to 10 kDa dextran were $(1.3 \pm 0.4) \times 10^{-6}$ cm s⁻¹, $(4.8 \pm 1.9) \times 10^{-6}$ cm s⁻¹, and $(5.1 \pm 1.3) \times 10^{-6}$ cm s⁻¹ for the three conditions, respectively; again, the addition of adipocytes led to higher permeability ($p < 0.01$), while insulin and Intralipid had no effect ($p = 0.97$, figure 3(F)).



3.3. Adipose tissues respond appropriately to lipogenic and lipolytic hormones

To examine the lipogenic response of vascularized adipose tissues, we switched some tissues to perfusion with media that contained insulin and Intralipid, starting on day 1. After four more days of perfusion, adipose tissues that were treated with insulin and Intralipid had clearly larger lipid droplets (figure 4(A)). The tissues showed a $72 \pm 18\%$ increase in lipid droplet area per cell over four days, which is higher than the $24 \pm 22\%$ increase in tissues that were perfused without lipogenic supplements ($p < 0.001$, figure 4(B)).

To examine the lipolytic response, we switched tissues that were previously perfused with insulin- and Intralipid-supplemented media to perfusion media with or without epinephrine, starting on day 5. After an additional four days of perfusion, tissues that were treated with epinephrine had shrunken lipid droplets (figure 4(C)); in contrast, tissues that were not perfused with epinephrine maintained their lipid droplets. Tissues that were perfused with epinephrine-supplemented media showed marked decrease ($-33 \pm 3\%$) in lipid droplet area per cell over four days ($p < 0.001$, compared to tissues perfused with media without epinephrine, figure 4(D)). Eventually, the lipid droplets in epinephrine-treated tissues regressed to a size similar to those on day 1 of perfusion, i.e., before lipogenic or lipolytic supplements were added.

3.4. Vascular perfusion supports a gradient of adipocyte lipogenesis in centimeter-scale tissues

To better understand how the separation between adipocytes and the vessel affects adipocyte function, we formed tissues that extended up to 10 mm away from the vessel wall with two adipocyte densities. In these tissues, after seven days of perfusion (the last six days with insulin and Intralipid), adipocytes that were near the microvessel appeared visibly larger compared to those that were further away from the vessel (figure 5(A)). In tissues that contained $10^6 \text{ cells ml}^{-1}$, adipocytes that were within 1 mm from the vessel showed a $115 \pm 21\%$ increase in lipid droplet area over six days, whereas adipocytes that were further than 9 mm away showed modest growth ($21 \pm 13\%$, figure 5(B)). In tissues that contained $1.5 \times 10^6 \text{ cells ml}^{-1}$, adipocytes that were within 1 mm from the vessel showed a $105 \pm 23\%$ increase over six days, whereas adipocytes that were further than 9 mm away showed essentially no growth (figure 5(C)). For both cell concentrations, most of the lipid accumulation occurred between days 1 and 5, with only little further growth from days 5 to 7.

4. Discussion

In this study, we engineered small-scale adipose tissues that contained perfusable microvessels. The tissues were formed by micromolding suspensions of differentiated 3T3-L1 adipocytes in type I collagen

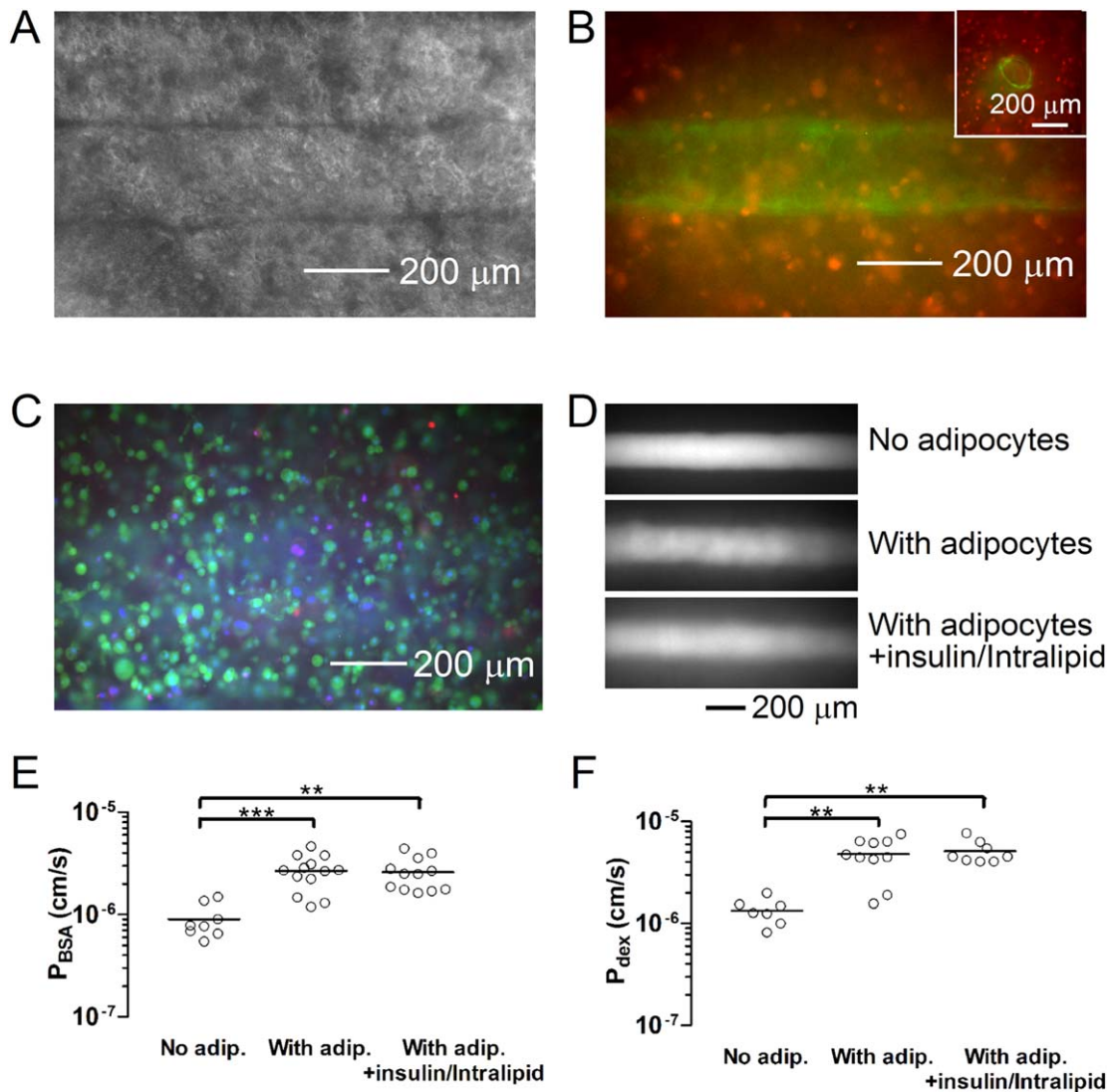


Figure 3. Structural and basic functional characterization of vascularized adipose tissues. (A) Phase-contrast image of vascularized tissue on day 3. (B) CD31 (green) and Nile Red (red) stain of endothelium and 3T3-L1 adipocytes, respectively. *Inset:* cross-sectional view. (C) Live cell (green), dead cell (red), and nuclei (blue) stain of adipose tissue on day 3. (D) Fluorescence images taken after twenty minutes of vascular perfusion with Alexa Fluor 594-conjugated BSA. (E) Vascular permeability coefficients to BSA (P_{BSA}). (F) Vascular permeability coefficients to 10 kDa dextran (P_{dex}). **, $p < 0.01$; ***, $p < 0.001$.

around an empty channel that subsequently served as a template for endothelialization. We found that adipocyte-laden collagen had ~40% lower stiffness and ~50% higher hydraulic permeability, compared to bare collagen gel. Although adding adipocytes to collagen reduced the collagen concentration, the change was small (~3%), and it is unlikely that the observed differences in physical properties can be explained primarily by the dependence of stiffness and hydraulic permeability on gel concentration. Remodeling of collagen by embedded adipocytes may contribute to the physical changes. Accumulation of lipid over a span of up to five days in culture did not appear to alter the mechanical properties of the formed tissues. The measured stiffness of adipocyte-laden collagen gel (~180 Pa) was lower than that of native subcutaneous adipose tissue (2–3 kPa) [25, 26], which is likely a result of the lower volume

fraction of adipocytes in the gels. The stiffness could potentially be improved by incorporating larger adipocytes (e.g., human white adipocytes) at higher concentration.

The flow rates and vessel diameters in the current study were larger than those measured for vessels in adipocyte-free gels from previous work [18], most likely because the adipocyte-containing gels were less stiff. Adding adipocytes to the collagen gel also resulted in a three-fold increase in vascular permeability to both BSA and 10 kDa dextran. This result can potentially be explained from the disruption of endothelial barrier function by free fatty acids [27] and by adipocyte-secreted permeability factors, such as vascular endothelial growth factor [28] and leptin [29]. The unevenness of the vascular profiles that we observed only in adipocyte-containing tissues may also have a permeability-enhancing effect. Differences in vascular

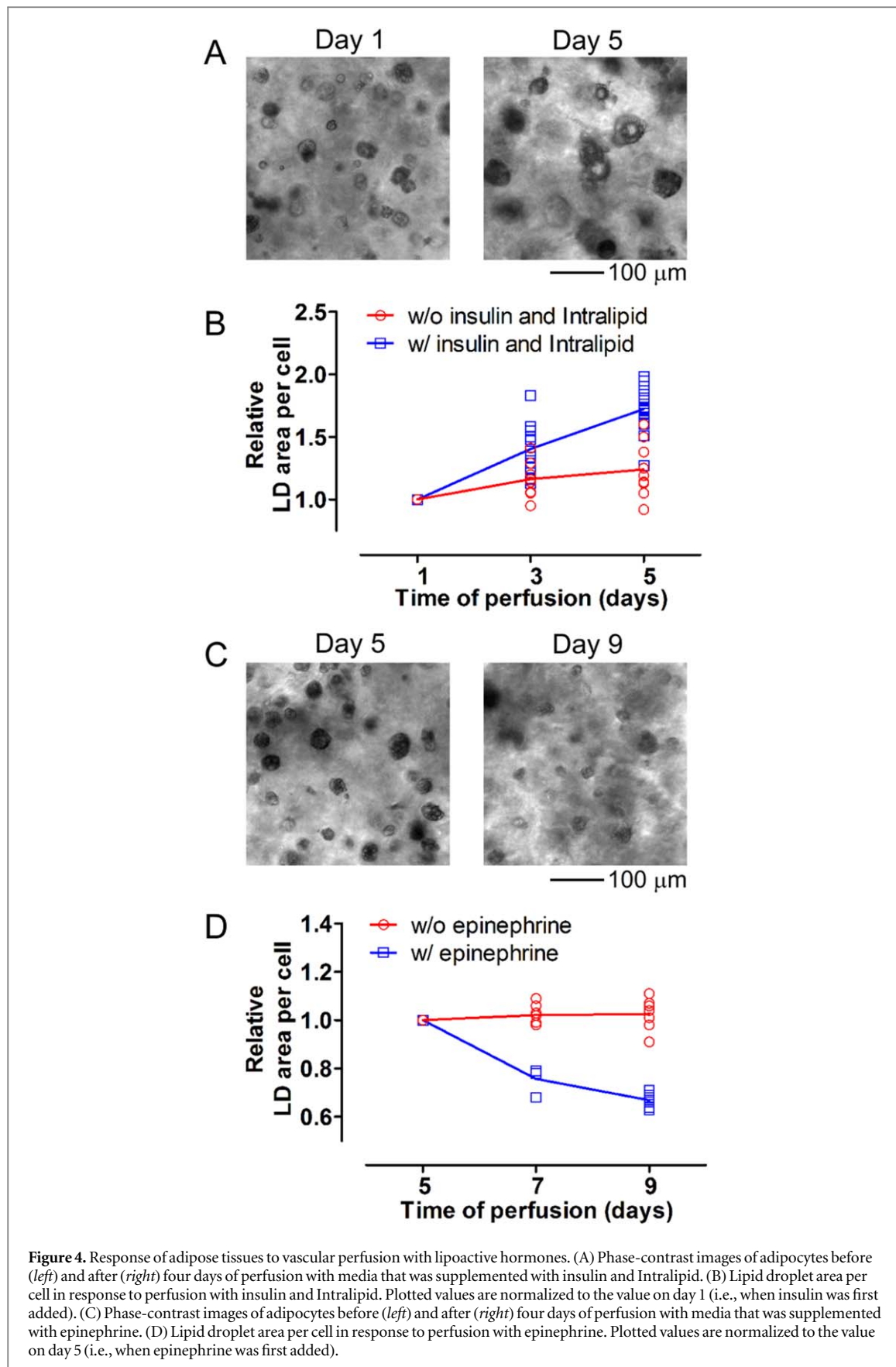


Figure 4. Response of adipose tissues to vascular perfusion with lipoactive hormones. (A) Phase-contrast images of adipocytes before (left) and after (right) four days of perfusion with media that was supplemented with insulin and Intralipid. (B) Lipid droplet area per cell in response to perfusion with insulin and Intralipid. Plotted values are normalized to the value on day 1 (i.e., when insulin was first added). (C) Phase-contrast images of adipocytes before (left) and after (right) four days of perfusion with media that was supplemented with epinephrine. (D) Lipid droplet area per cell in response to perfusion with epinephrine. Plotted values are normalized to the value on day 5 (i.e., when epinephrine was first added).

shear stress, which can alter solute permeability [24], are unlikely to be responsible here; from the measured flow rates, we estimated the average vascular shear stress to be $\sim 12 \text{ dyn cm}^{-2}$ in adipocyte-containing

samples and $\sim 13 \text{ dyn cm}^{-2}$ in adipocyte-free samples. The measured vascular permeability in adipocyte-laden gel was comparable to mammalian venules of similar size ($\sim 2 \times 10^{-6} \text{ cm s}^{-1}$) [30].

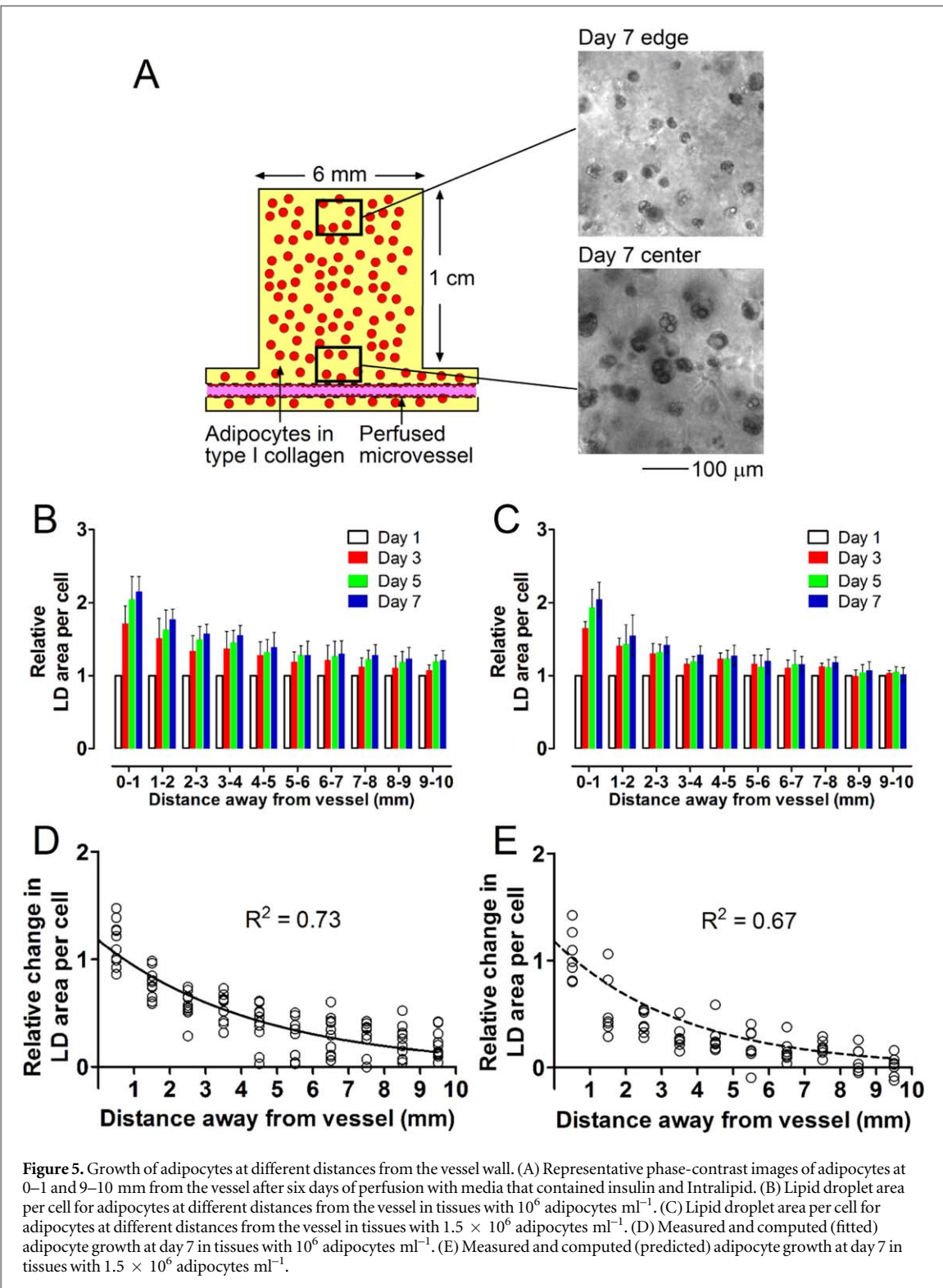


Figure 5. Growth of adipocytes at different distances from the vessel wall. (A) Representative phase-contrast images of adipocytes at 0–1 and 9–10 mm from the vessel after six days of perfusion with media that contained insulin and Intralipid. (B) Lipid droplet area per cell for adipocytes at different distances from the vessel in tissues with 10^6 adipocytes ml^{-1} . (C) Lipid droplet area per cell for adipocytes at different distances from the vessel in tissues with 1.5×10^6 adipocytes ml^{-1} . (D) Measured and computed (fitted) adipocyte growth at day 7 in tissues with 10^6 adipocytes ml^{-1} . (E) Measured and computed (predicted) adipocyte growth at day 7 in tissues with 1.5×10^6 adipocytes ml^{-1} .

Insulin increases lipid accumulation in adipocytes through multiple pathways, including enhancing the conversion of circulating triacylglycerol to fatty acid [15] and increasing the uptake of free fatty acid by adipocytes [14]. Conversely, epinephrine accelerates the breakdown of stored triglyceride into free fatty acids during periods of high energy demand such as fasting or exercise [31]. Both hormones are important mediators of metabolic conditions such as obesity and diabetes. It is therefore important to show that

engineered adipose tissue can respond appropriately to lipoactive hormones with lipogenesis or lipolysis. While many previous studies used either total lipid content [21, 32] or lipid droplet diameter [33] as a measure of lipid accumulation, neither method is suitable for the current study. The first method requires lysing the cells to release stored triglyceride, which prevents tracking adipocyte growth over time in the same sample. The second method is best-suited for unilocular adipocytes such as mature human white

adipocytes and not for multilocular 3T3-L1 cells. We therefore measured change in lipid droplet area per cell as an indicator of lipogenesis and lipolysis.

We observed ~70% increase in lipid droplet area per cell in adipose tissue after four days of perfusion with insulin and Intralipid, whereas adipose tissue perfused without insulin and Intralipid only showed a ~25% increase. While the effects of insulin and Intralipid were not studied separately, our findings indicate that the engineered adipose tissues responded to lipogenic compounds with increased lipid accumulation. Similarly, adipose tissues that were previously ‘fattened’ with insulin and Intralipid showed ~30% decrease in lipid droplet area per cell upon removal of insulin/Intralipid and addition of epinephrine for four days, which is consistent with the lipolytic action of epinephrine. When switched to media that did not contain lipogenic or lipolytic compounds, adipocytes that were prefed with insulin and Intralipid neither shrunk nor showed further growth.

In wide adipose tissues that were fed by a single microvessel, adipocytes that were within 0–1 mm from the vessel showed roughly two-fold growth over six days in tissues at both high (1.5×10^6 cells ml $^{-1}$) and low (10^6 cells ml $^{-1}$) cell densities. The lipid accumulation was less for adipocytes that were further away from the vessel; for adipocytes that were the furthest (9–10 mm) from the vessel, little accumulation of lipid was observed. In low-density tissues, adipocytes that were 9–10 mm away from the vessels showed ~20% growth. In high-density tissues, virtually no growth was observed in adipocytes that were 9–10 mm away from the vessel. Most of the lipid accumulation occurred in the first four days of perfusion with lipogenic supplements.

The plots of lipid accumulation versus distance suggest that diffusive transport of a lipogenic signal from the vessel to adipocytes far from the vessel was limited by consumption of the signal by adipocytes that were close to the vessel. We used a simple Krogh-type model to rationalize these plots. In this model, we assume that the lipogenic nutrient was taken up by adipocytes with first-order kinetics as it diffused from the vessel into the tissue. We also assume that lipid droplet accumulation was metabolized with first-order kinetics. The underlying equations for lipid accumulation are:

$$\frac{\partial C}{\partial t} = D \frac{\partial^2 C}{\partial x^2} - \rho k_{up} C, \quad (3)$$

$$\frac{\partial G}{\partial t} = k_{prod} C - BG, \quad (4)$$

where C is the concentration of lipogenic factors (insulin, Intralipid, etc) in the extracellular space, x is the distance away from the vessel, ρ is the density of adipocytes in the tissue, k_{up} is the uptake rate of lipogenic factors by adipocytes, G is the accumulation of lipid, k_{prod} is the rate at which adipocytes accumulate lipid in response to the lipogenic signal, and B is

the rate at which adipocytes metabolize accumulated lipid. This model predicts that the steady-state lipid accumulation also decreases exponentially with distance, with a decay length that is inversely proportional to $\rho^{1/2}$:

$$G \propto e^{-\sqrt{\frac{\rho k_{up}}{D}}x}. \quad (5)$$

An exponential fit to the day 7 lipid accumulation in tissues with 10^6 3T3-L1 cells ml $^{-1}$ yielded $\sqrt{\frac{\rho k_{up}}{D}} = 0.23$ mm $^{-1}$, with a goodness-of-fit $R^2 = 0.73$ (figure 5(D)). We then used equation (5) to predict the lipid accumulation profile of tissues with 1.5×10^6 3T3-L1 cells ml $^{-1}$ by using the fitted coefficients and multiplying ρ by 1.5. The resulting curve yielded $R^2 = 0.67$ (figure 5(E)). The reasonable agreement between experimental data and this model provides a quantitative tool to predict the lipid accumulation profile in adipose tissues that contain more complex vascular geometries, even without knowledge of the rate-limiting lipogenic factor or the metabolic constants.

5. Conclusion

We have described a method for engineering lipoactive adipose tissue with pre-patterned vasculature that allows immediate perfusion. Our design can accommodate both vascular and non-vascular cell types, and we believe it can serve as a building block for constructing larger tissues for potential future application in soft-tissue repair. The current tissue can be used as a ‘fat-on-a-chip’ microphysiological system to model vessel-adipocyte interactions. It can also be incorporated as one element of more complex adipose-rich tissues, such as in models of breast tumors [34]. To scale up the current tissue into a clinically implantable flap, we will need to modify these tissues so that they use primary human adipocytes or adipose-derived stem cells, a branching vascular network that can support large tissues, and a robust vascular pedicle that can withstand suture anastomosis and perfusion at arterial pressures [35].

Acknowledgments

We thank Celeste Nelson for providing 3T3-L1 cells, Usman Ghani for experimental assistance, and Matthew Layne for helpful discussions. This work was supported by the National Institute of Biomedical Imaging and Bioengineering (award EB018851), the National Cancer Institute (award CA214292), and the NIH Translational Research in Biomaterials training program (award EB006359), and by the Undergraduate Research Opportunities Program (to JX, CTN, and MWM) and Lutchen Fellowship (to MWM) at Boston University. CTN was supported by a Summer Term Alumni Research Scholarship at Boston University.

ORCID iDs

- Tyler J Ryan  <https://orcid.org/0000-0003-2506-8901>
Joe Tien  <https://orcid.org/0000-0003-4283-3986>

References

- [1] Levin LS 2008 Principles of definitive soft tissue coverage with flaps *J. Orthop. Trauma* **22** S161–6
- [2] Choi J H, Gimble J M, Lee K, Marra K G, Rubin J P, Yoo J J, Vunjak-Novakovic G and Kaplan D L 2010 Adipose tissue engineering for soft tissue regeneration *Tissue Eng. B* **16** 413–26
- [3] Patrick C W Jr 2000 Adipose tissue engineering: the future of breast and soft tissue reconstruction following tumor resection *Semin. Surg. Oncol.* **19** 302–11
- [4] Pattani K M, Byrne P, Boahene K and Richmon J 2010 What makes a good flap go bad? A critical analysis of the literature of intraoperative factors related to free flap failure *Laryngoscope* **120** 717–23
- [5] Suominen S and Asko-Seljavaara S 1995 Free flap failures *Microsurgery* **16** 396–9
- [6] Billings E Jr and May J W Jr 1989 Historical review and present status of free fat graft autotransplantation in plastic and reconstructive surgery *Plast. Reconstr. Surg.* **83** 368–81
- [7] Ersek R A 1991 Transplantation of purified autologous fat: a 3 year follow-up is disappointing *Plast. Reconstr. Surg.* **87** 219–27
- [8] Kawaguchi N, Toriyama K, Nicodemou-Lena E, Inou K, Torii S and Kitagawa Y 1998 *In vivo* adipogenesis in mice at the site of injection of basement membrane and basic fibroblast growth factor *Proc. Natl Acad. Sci. USA* **95** 1062–6
- [9] Abbott R D, Wang R Y, Reagan M R, Chen Y, Borowsky F E, Zieba A, Marra K G, Rubin J P, Ghobrial I M and Kaplan D L 2016 The use of silk as a scaffold for mature, sustainable unilocular adipose 3D tissue engineered systems *Adv. Healthcare Mater.* **5** 1667–77
- [10] Kimura Y, Ozeki M, Inamoto T and Tabata Y 2003 Adipose tissue engineering based on human preadipocytes combined with gelatin microspheres containing basic fibroblast growth factor *Biomaterials* **24** 2513–21
- [11] Rophael J A, Craft R O, Palmer J A, Hussey A J, Thomas G P, Morrison W A, Pennington A J and Mitchell G M 2007 Angiogenic growth factor synergism in a murine tissue engineering model of angiogenesis and adipogenesis *Am. J. Pathol.* **171** 2048–57
- [12] Koopman R, Schaart G and Hesselink M K 2001 Optimisation of oil red O staining permits combination with immunofluorescence and automated quantification of lipids *Histochem. Cell Biol.* **116** 63–8
- [13] Duncan R E, Ahmadian M, Jaworski K, Sarkadi-Nagy E and Sul H S 2007 Regulation of lipolysis in adipocytes *Annu. Rev. Nutrition* **27** 79–101
- [14] Stahl A, Evans J G, Pattel S, Hirsch D and Lodish H F 2002 Insulin causes fatty acid transport protein translocation and enhanced fatty acid uptake in adipocytes *Dev. Cell* **2** 477–88
- [15] Knutson V P 2000 The release of lipoprotein lipase from 3T3-L1 adipocytes is regulated by microvessel endothelial cells in an insulin-dependent manner *Endocrinology* **141** 693–701
- [16] Chernick S S, Spooner P M, Garrison M M and Scow R O 1986 Effect of epinephrine and other lipolytic agents on intracellular lipolysis and lipoprotein lipase activity in 3T3-L1 adipocytes *J. Lipid Res.* **27** 286–94
- [17] Choi J H, Bellas E, Gimble J M, Vunjak-Novakovic G and Kaplan D L 2011 Lipolytic function of adipocyte/endothelial cocultures *Tissue Eng. A* **17** 1437–44
- [18] Chrobak K M, Potter D R and Tien J 2006 Formation of perfused, functional microvascular tubes *in vitro* *Microvasc. Res.* **71** 185–96
- [19] Zebisch K, Voigt V, Wabitsch M and Brandsch M 2012 Protocol for effective differentiation of 3T3-L1 cells to adipocytes *Anal. Biochem.* **425** 88–90
- [20] Chan K L S, Khankhel A H, Thompson R L, Coisman B J, Wong K H K, Truslow J G and Tien J 2014 Crosslinking of collagen scaffolds promotes blood and lymphatic vascular stability *J. Biomed. Mater. Res. A* **102** 3186–95
- [21] Spooner P M, Chernick S S, Garrison M M and Scow R O 1979 Development of lipoprotein lipase activity and accumulation of triacylglycerol in differentiating 3T3-L1 adipocytes. Effects of prostaglandin F₂ α , 1-methyl-3-isobutylxanthine, prolactin, and insulin *J. Biol. Chem.* **254** 1305–11
- [22] Price G M and Tien J 2011 Methods for forming human microvascular tubes *in vitro* and measuring their macromolecular permeability *Methods Mol. Biol.* **671** 281–93
- [23] Truslow J G and Tien J 2013 Determination of vascular permeability coefficients under slow luminal filling *Microvasc. Res.* **90** 117–20
- [24] Price G M, Wong K H, Truslow J G, Leung A D, Acharya C and Tien J 2010 Effect of mechanical factors on the function of engineered human blood microvessels in microfluidic collagen gels *Biomaterials* **31** 6182–9
- [25] Alkhouri N et al 2013 The mechanical properties of human adipose tissues and their relationships to the structure and composition of the extracellular matrix *Am. J. Physiol. Endocrinol. Metab.* **305** E1427–35
- [26] Samani A, Zubovits J and Plewes D 2007 Elastic moduli of normal and pathological human breast tissues: an inversion-technique-based investigation of 169 samples *Phys. Med. Biol.* **52** 1565–76
- [27] Hennig B, Ramasamy S, Alvarado A, Shantha N C, Boissonneault G A, Decker E A and Watkins B A 1993 Selective disruption of endothelial barrier function in culture by pure fatty acids and fatty acids derived from animal and plant fats *J. Nutrition* **123** 1208–16
- [28] Fukumura D, Ushiyama A, Duda D G, Xu L, Tam J, Krishna V, Chatterjee K, Garkavtsev I and Jain R K 2003 Paracrine regulation of angiogenesis and adipocyte differentiation during *in vivo* adipogenesis *Circ. Res.* **93** e88–97
- [29] Cao R, Brakenhielm E, Wahlestedt C, Thyberg J and Cao Y 2001 Leptin induces vascular permeability and synergistically stimulates angiogenesis with FGF-2 and VEGF *Proc. Natl Acad. Sci. USA* **98** 6390–5
- [30] Yuan Y, Chilian W M, Granger H J and Zawieja D C 1993 Permeability to albumin in isolated coronary venules *Am. J. Physiol.* **265** H543–52
- [31] Nielsen T S, Jessen N, Jorgensen J O, Moller N and Lund S 2014 Dissecting adipose tissue lipolysis: molecular regulation and implications for metabolic disease *J. Mol. Endocrinol.* **52** R199–222
- [32] Fischbach C, Spruss T, Weiser B, Neubauer M, Becker C, Hacker M, Gopferich A and Blunk T 2004 Generation of mature fat pads *in vitro* and *in vivo* utilizing 3D long-term culture of 3T3-L1 preadipocytes *Exp. Cell Res.* **300** 54–64
- [33] Varlamov O, Somwar R, Cornea A, Kievit P, Grove K L and Roberts C T Jr 2010 Single-cell analysis of insulin-regulated fatty acid uptake in adipocytes *Am. J. Physiol. Endocrinol. Metab.* **299** E486–96
- [34] Cozzo A J, Fuller A M and Makowski L 2017 Contribution of adipose tissue to development of cancer *Compr. Physiol.* **8** 237–82
- [35] Li X, Xu J, Nicolescu C T, Marinelli J T and Tien J 2017 Generation, endothelialization, and microsurgical suture anastomosis of strong 1 mm diameter collagen tubes *Tissue Eng. A* **23** 335–44